Acta Chemica Scandinavica, 1994: 48: 1–11
Printed in Belgium – all rights reserved

ACTA
CHEMICA SCANDINAVICA
ISSN 0904-213X

Study of Adsorption and Ion-Exchange Properties of Some Porous Membranes

Kyösti Kontturi,* Aki Savonen† and Mikko Vuoristo

Helsinki University of Technology, Laboratory of Physical Chemistry and Electrochemistry, Kemistintie 1, SF-02150 Espoo, Finland

Kontturi, K., Savonen, A. and Vuoristo, M., 1994. Study of Adsorption and Ion-Exchange Properties of Some Porous Membranes. – Acta Chem. Scand. 48: 1–11. © Acta Chemica Scandinavica 1994.

Adsorption of ions and ion-exchange properties of three different types of polymeric microfiltration membranes (with pore sizes of 0.1–8 μm) were studied by measuring the streaming potential and transport numbers in different electrolyte concentrations. A completely computerized apparatus for the measuring of the streaming potential, allowing a fast and accurate determination of the streaming potential as well as the study of slow adsorption kinetics, was built. The transport number in the membrane was determined by measuring the electromotive force in a cell with transference. The rotating diffusion cell was employed to overcome the problem created by the polarization layers.

The measured data were used to estimate the surface charge density and the pore radius of the membrane in the swollen state. Furthermore, an effort to study the protein adsorption by both methods was made.

The results clearly show that chloride ions are adsorbed on the pore wall, creating cation-exchange properties for the membrane. However, owing to the large pore size, only in dilute electrolyte solutions ($\leqslant 10^{-3}$ M) did the transport number in the membrane deviate from its value in water. The protein cytochrome c is evidently adsorbed by a hydrophobic interaction, increasing the number of charges on the pore wall. This behaviour indicates that only a monolayer of adsorbed species is formed on the surface of the pores.

Recently, a method to separate small ions[1–9] and polyelectrolytes[10] based on a transport process in a porous membrane has been presented and extensively studied. Also, a method to determine the effective charge numbers and ionic diffusion coefficients of a polyelectrolyte, resorting to the convective diffusion process across a wide-pore membrane, has been investigated.[11–18] The modelling of these procedures utilizes the inert character of wide-pore membranes, i.e. the role of adsorption in the form of a hydrophobic interaction and the role of ion-exchange properties due to the adsorbed ions can be neglected.

However, it has recently been shown that anions such as chloride ions are significantly adsorbed onto certain polymeric matrices, creating ion-exchange properties.[19] These properties can, if the solutions are sufficiently dilute, cause the porous membrane to act as an ion-exchange membrane. Furthermore, many polyelectrolytes such as proteins may be adsorbed on the wall of the pore, fouling the membrane.

In this paper we consider the ion-exchange properties of some commercial porous membranes by measuring the streaming potential and transport number with the aid of electromotive force measurements in a nonhomogeneous system. The pore sizes of the membranes studied vary from 0.1 to 8 μm.

Choice of experimental methods

Our main interest is to obtain information about the behaviour of electrolytes and polyelectrolytes (proteins) relevant to adsorption and to the modelling of transport processes (diffusion and migration) inside the membrane. Therefore, suitable parameters to be measured are the cation transport number of the base electrolyte in the membrane (t_+^M) and the surface charge density (q_2).

The transport number in the membrane can be directly measured in a cell with transference by the electromotive force, here called the EMF method. The problem with the EMF method is the non-homogeneous electrolyte system involved, which results in concentration polarization at the membrane surfaces. This effect cannot be neglected because of the high porosity of the porous membranes of interest. Fortunately, there are ways to deal with the

* To whom correspondence should be addressed.
† Present address: J. W. Suominen Oy, SF-29251 Nakkila, Finland.

thicknesses of polarization layers, and thus the diffusion processes in these layers are under control. However, the diffusion processes inside the membrane present some problems because of the changes in the thickness of the double layer and the surface charge density due to the concentration changes along the capillary pore of the membrane.

The surface charge density q_2 is indirectly accessible by measuring the streaming potential. This means that a microscopic model to evaluate q_2 is needed. Furthermore, well established studies[19–21] have shown that a relatively simple microscopic theory can be applied to determine q_2. In addition, some hints of the validity of this approach can also be obtained from our measurement of t_+^M by applying a microscopic treatment to this quantity.

Theoretical

The membrane is considered as an array of pores with adsorbed charges on the pore wall. The surface charge density q_2 of a pore in the membrane will affect the transport process across the membrane. The transport quantities of a charged membrane (transport numbers and diffusion coefficients) are generally different from the ones in the corresponding electrolyte solution. This is due to the changes in concentrations and the presence of electrical double layer causing a radial gradient of ionic concentrations inside the pore. Therefore, the diffusion and migration processes inside the porous membrane with ion-exchange properties are studied first.

Let us assume that we are dealing with a membrane having cation-exchange properties, that the contribution of the surface migration to the transport process is negligible (i.e. the Debye length is considerably smaller than the pore radius), and that the effect of surface charge can be included in the model through the condition of electroneutrality. The Nernst–Planck equation, without the convective term, for a strong 1,1-electrolyte system is

$$-J_+ = D_+ \frac{d\bar{c}_+}{dx} + D_+ \bar{c}_+ f \frac{d\phi}{dx} \tag{1}$$

$$-J_- = D_- \frac{d\bar{c}_-}{dx} - D_- \bar{c}_- f \frac{d\phi}{dx} \tag{2}$$

where x is a spatial coordinate along the pore axis, D_+ and D_- are ionic diffusion coefficients of cation and anion, $\bar{c}_+$ and $\bar{c}_-$ are ionic concentrations inside the membrane, ϕ is the electrical potential, and $f = F/RT$. $\bar{c}_+$, $\bar{c}_-$ and ϕ are taken as average values with respect to the radial coordinate of a pore. The relationship of fluxes (J_+, J_-) and electric current density (I) are related by

$$J_+ - J_- = I/F \tag{3}$$

and the condition of electroneutrality is

$$\bar{c}_+ - \bar{c}_- - c_M = 0 \tag{4}$$

where c_M is the concentration of fixed charges per unit volume of the pore. With the aid of eqns. (1)–(4) we can solve the problem. Let us find expressions for the diffusion coefficient $(D_\pm^M)$ and the transport numbers (t_-^M, t_+^M) in the membrane. Assuming that c_M = constant i.e. $dc_M/dx = 0$, we can derive eqn. (5) (by eliminating $d\phi/dx$ and realizing that the diffusional contribution must be taken with respect to the gradient of $\bar{c}_-$) in the form:

$$-J_- = D_\pm^M \frac{d\bar{c}_-}{dx} + t_-^M \frac{I}{F} \tag{5a}$$

where

$$D_\pm^M = \frac{D_+ D_- (2\bar{c}_- + c_M)}{D_- \bar{c}_- + D_+ \bar{c}_- + D_+ c_M} \tag{5b}$$

$$t_-^M = \frac{D_- \bar{c}_-}{D_- \bar{c}_- + D_+ \bar{c}_- + D_+ c_M} \tag{5c}$$

$$\kappa = f(D_- \bar{c}_- + D_+ \bar{c}_- + D_+ c_M) \tag{5d}$$

where κ is the conductivity. Owing to the basic assumptions of the Nernst–Planck equation[22] the diffusion coefficients and transport numbers are given in the solvent-fixed (i.e. Hittorf) reference system. Using eqn. (5d) we can write eqn. (5c) as

$$t_-^M = \frac{fD_- \bar{c}_-}{\kappa} \Rightarrow t_+^M = 1 - t_-^M = \frac{fD_+ \bar{c}_+}{\kappa} \tag{6}$$

The problem is the fact that the concentrations involved in the above equations are those in the membrane, and usually we know only the concentrations outside the membrane, i.e. the bulk concentrations of the aqueous phases. To solve this problem Donnan equilibrium has to be considered. Donnan stated that the electrochemical potentials in aqueous and membrane phases are equal for each ion. When the activity coefficients are taken to be same in the aqueous and membrane phases, the Donnan treatment leads in our case to

$$\bar{c}_+ \bar{c}_- = c_+ c_-$$

where c_+ and c_- are the ionic concentration in the aqueous phase. Since $c_+ = c_-$ we obtain

$$\bar{c}_+ = \frac{c_+}{(1-\theta)^{1/2}} \tag{7a}$$

$$\bar{c}_- = c_+ (1-\theta)^{1/2} \tag{7b}$$

where $\theta = c_M/\bar{c}_+$. If θ can be measured, the concentrations $(\bar{c}_+, \bar{c}_-)$ in the membrane phase are known. By rearranging eqns. (5c) and (6) we obtain

$$\frac{c_M}{\bar{c}_+} = \theta = -\frac{D_+}{D_-}\left(\frac{1}{t_+^M} - \frac{1}{t_+}\right) \tag{8}$$

where the transport number of the cation in water is given by $t_+ = D_+/(D_+ + D_-)$. Thus θ can be calculated after

measuring t_+^M (t_+ is known from the literature). The value of θ varies from zero to unity depending on the ion-exchange ability of the membrane.

Surface charge density by streaming potential. Electrokinetic measurements are carried out in isothermal conditions without concentration differences in the axial direction of the capillary pore of a membrane. In that case the electric current (i) and volume flow rate (Q) of the solution through one pore are chosen as independent generalized fluxes. The corresponding forces are electric field (E_x) and pressure gradient (dp/dx) in axial direction x. These forces are assumed to be constant throughout the membrane.

With the aid of a microscopic model for a charged membrane, the phenomenological coefficients can be expressed as functions of the surface charge density q_2, which is defined as the charge of a unit area of the pore wall and has the same sign as the immobile charge. To take into account the anisotropy of the membrane in the microscopic model some assumptions about pore geometry should be made. Here each pore is taken as a long cylindrical capillary which is in contact with two bulk solutions of equal composition and temperature. The linear force–flux equations are obtained by solving the Navier–Stokes equation for momentum balance, the Nernst–Planck equation for convective migration and the linearized Poisson–Boltzmann equation for the electrostatic space-charge distribution in a charged capillary:[20]

$$\frac{i}{\pi r_0^2} = \left\{ \kappa_{avg} + \frac{q_2^2}{\mu}\left[1 - \frac{I_0(R_0)\, I_2(R_0)}{I_1^2(R_0)}\right]\right\} E_x + \frac{q_2 \lambda}{\mu} \frac{I_2(R_0)}{I_1(R_0)} \frac{dp}{dx} \tag{9}$$

$$\frac{Q}{\pi r_0^2} = \frac{-\lambda q_2}{\mu} \frac{I_2(R_0)}{I_1(R_0)} E_x - \frac{r_0^2}{8\mu} \frac{dp}{dx} \tag{10}$$

where r_0 is the pore radius, μ is the viscosity of the solution and I_n is a modified Bessel function of order n. R_0 is a dimensionless pore radius, $R_0 = r_0/\lambda$, where the Debye length is defined by

$$\lambda = \left(\frac{\varepsilon RT}{F^2 \sum_i z_i^2 c_i^0} \right)^{1/2} \tag{11}$$

and the conductivity κ_{avg} is

$$\kappa_{avg} = \kappa^0 \left\{ 1 - \frac{q_2 F \lambda}{\varepsilon RT} \left[\frac{2}{R_0} - \frac{1}{I_1(R_0)} \right] \frac{\sum z_i^3 u_i c_i^0}{\sum z_i^2 u_i c_i^0} \right\} \tag{12}$$

$$\kappa^0 = F^2 \sum_i z_i^2 u_i c_i^0 \tag{13}$$

where ε is the permittivity of the solution, κ^0 and c_i^0 are the conductivity and concentration in the pore axis, u_i is the mobility, and z_i is the charge number. The subscript i refers to all mobile ions in solution.

The validity of this model is limited by linearization of the Boltzmann distribution for the case of low electrostatic potentials (i.e. when $R_0 \gg 1$ and surface charge densities are low). The assumption of uniform q_2 introduces some inaccuracy at high electrolyte concentrations and at small values of q_2 because the thickness of double layer is less than the mean distance between adsorbed ions or charged groups on the surface, giving rise to the discrete nature of the charges.

The measurable forces for the electrokinetic experiment are directly proportional to the pressure difference Δp and potential difference ΔU between bulk solutions. These can be obtained, when the pressure gradient and electric field are assumed to be constant, by integration over the pore length:

$$\Delta U = \int_0^l E_x \, dx = E_x l \qquad \Delta p = \int_0^l \frac{dp}{dx} dx = \frac{dP}{dx} l \tag{14}$$

where l is the effective thickness of the membrane. The total electric current I_m and flow rate through the membrane J_m can be expressed using effective area A^M of the membrane:

$$I_m = \frac{i}{\pi r_0^2} A^M \qquad J_m = \frac{Q}{\pi r_0^2} A^M \tag{15}$$

The phenomenological equations (9) and (10), together with eqns. (14) and (15) for measurable quantities, give us the basis for choosing a method for determination of surface charge density. In electrokinetic measurements one of the forces or fluxes is eliminated according to the experimental conditions, and the slope between the two remaining quantities is measured, e.g. q_2 can be obtained by putting $i = 0$ in eqn. (9) and determining the slope of potential–pressure curve. Strictly speaking, in the case of highly porous membrane the contribution of the pressure difference to the flow rate is difficult to eliminate; e.g. in the electro-osmotic measurement the volume flow is measured, which in turn creates a pressure difference.

In the electrokinetic measurements an important aspect is the membrane constant (l/A^M). If an electrokinetic phenomenon is studied by measuring a force with respect to a flux or *vice versa*, l/A^M must be known. In practice this means that the membrane constant is to be determined in a separate measurement. However, if the electrokinetic phenomenon is investigated by measuring one force (flux) with respect to another force (flux), the membrane constant does not appear in the equation. Thus l/A^M must be known when electrokinetic phenomena such as second streaming current ($I_m/\Delta p$, $\Delta U = 0$), second electro-osmotic flow ($J_m/\Delta U$, $\Delta p = 0$), second streaming potential ($\Delta U/J_m$, $I_m = 0$) or second electro-osmotic pressure ($\Delta p/I_m$, $J_m = 0$) are dealt with. However, the membrane constant need not be known e.g. in the case of streaming potential ($\Delta U/\Delta p$, $I_m = 0$), electro-osmotic pressure ($\Delta p/\Delta U$, $J_m = 0$) and electro-osmotic flow (J_m/I_m, $\Delta p = 0$).

For these experimental reasons the streaming potential measured as function of pressure difference seems to be the most straightforward way to estimate surface charge density of a microporous membrane. Imposing the condition of zero electric current the characteristic equation for the streaming potential measurement can be obtained from eqns. (9) and (11)–(15):

$$\frac{\Delta U}{\Delta p} = \frac{E_x l}{(\mathrm{d}p/\mathrm{d}x)l} = \frac{-q_2 \lambda}{\mu \kappa_{\mathrm{eff}}} \frac{I_2(R_0)}{I_1(R_0)} \tag{16}$$

$$\kappa_{\mathrm{eff}} = \kappa_{\mathrm{avg}} + \frac{q_2^2}{\mu}\left(1 - \frac{I_0(R_0)\, I_2(R_0)}{I_1^2(R_0)}\right) \tag{17}$$

From eqns. (9) and (17) one can see that κ_{eff} is the effective conductivity of the solution in a charged capillary at constant pressure.

When $R_0 \gg 1$ the solution in the pore axis is electroneutral, and κ^0 is equal to the bulk solution conductivity. Thus q_2 can be found iteratively according to eqns. (16) and (17) without a separate measurement for κ_{eff}. Because of the q_2^2-dependent term in eqn. (17) we get two different q_2 values for each measured value of $\Delta U/\Delta p$. The root having higher absolute value gives unreasonably high membrane conductivities and must be rejected.

Streaming potential is a convenient technique in studying membranes with a wide range of pore sizes and solution conductivities. The relationship between streaming potential and surface charge density is almost independent of pore size when $R_0 \geqslant 10$, which is an important feature because pore sizes and their distributions are rarely well characterized in various swollen states of the membrane.

Transport number in a porous membrane by the EMF method. The transport number of a cation in a membrane, t_+^{M}, can be obtained from the EMF measurement in a cell with transference having a binary electrolyte system on both sides of the junction. This procedure is called here the EMF method. The type of cell we used was

transition region

ε		α	‖			‖	β		ε′
Ag(s)|AgCl(s)|		KCl	‖	|M|		‖	KCl	|AgCl(s)|Ag(s)
|		|(in water)‖				‖	(in water)|	|
			α	0		l	β		

(18)

in which the transition region consists of two polarization layers of thickness δ and a porous microfiltration membrane of thickness l. If we take the current density to be zero the cell potential E, the EMF becomes

$$-FE = t_+^{\mathrm{w}} \int_{\alpha}^{0} \mathrm{d}\mu_{\pm} + t_+^{\mathrm{M}} \int_{0}^{l} \mathrm{d}\mu_{\pm} + t_+^{\mathrm{w}} \int_{l}^{\beta} \mathrm{d}\mu_{\pm} \tag{19}$$

where t_+^{w} is the cation transference number in both the α- and β-phases and t_+^{M} is the cation transference number in the membrane. Both transport numbers are presented in a solvent fixed (i.e. Hittorf) reference system. The concentration dependence of the transport numbers in each measurement is assumed to be negligible. F is the Faraday constant and $\mu_{\pm}$ is chemical potential of the base electrolyte.

The problem that arises in the EMF method is the concentration polarization in the diffusion layers. In this work a rotating diffusion cell[23] has been used to overcome this problem. The theoretical basis of the rotating diffusion cell is the same as that for a rotating disc electrode. It is well known that the diffusion layer thickness δ (in cm) is given by the Levich equation:

$$\delta = 1.612 D^{1/3} \nu^{1/6} \omega^{-1/2} \tag{20}$$

where D is the salt diffusion coefficient (in $\mathrm{cm^2\,s^{-1}}$), ν is the kinematic viscosity (in $\mathrm{cm^2\,s^{-1}}$) and ω is the rotation speed (in $\mathrm{rad\,s^{-1}}$). The membrane is again assumed to consist of circular cylindrical pores with radius r_0 and length l, and $l \gg r_0$ (Fig. 1). The charge density per unit area on the pore wall is q_2.

A key feature of the model described here is the concept of a hypothetical surface phase in which only counter-ions exist. This thinking results from the fact that diffusion occurs only in bulk solution inside the pore. Cation concentration in the surface phase is c_+^{s} (calculated with respect to the total volume of the pore) and respectively in the bulk phase of the membrane c_+^{B} (Fig. 1). Hence the total concentration of cation $\bar{c}_+$ in the membrane is

$$\bar{c}_+ = c_+^{\mathrm{B}} + c_+^{\mathrm{S}} \tag{21}$$

In the bulk phase inside the pore the condition of electroneutrality exists:

$$\bar{c}_- = c_+^{\mathrm{B}} \tag{22}$$

In a condition of zero electric current, the cation flux in the membrane is given by Fick's first law of diffusion:

$$J_+ A^{\mathrm{M}} = -D_{\pm}^{\mathrm{M}} A^{\mathrm{M}} \frac{\mathrm{d}c_+^{\mathrm{B}}}{\mathrm{d}x} \tag{23}$$

where $D_{\pm}^{\mathrm{M}}$ is the average diffusion coefficient of the base

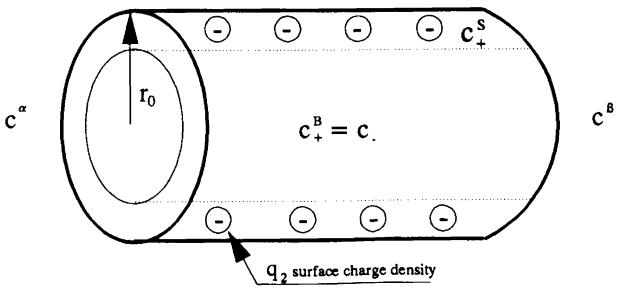

Fig. 1. A schematic drawing of one pore of length l and radius r_0 in the membrane. The surface charge density q_2 on the pore wall is assumed to be uniform. The dotted line separates bulk pore solution of cation concentration c_+^{B} from surface phase at counter-ion concentration c_+^{s}.

electrolyte in the membrane [eqn. (5a)] and A^M is the effective cross-sectional area of the pores. Integration yields

$$J_+ A^M = \frac{D_\pm^M A^M}{l} [c_+^B(x=0) - c_+^B(x=l)] \quad (24)$$

The transport equations in diffusion layers are

$$J_+ A^w = \frac{D_\pm^w A^w}{\delta} [c_+^\alpha - c_+^\alpha(x=0)]$$

$$= \frac{D_\pm^w A^w}{\delta} [c_+^\beta(x=l) - c_+^\beta] \quad (25)$$

where δ is the thickness of the polarization layers, $D_\pm^w$ is the diffusion coefficient in the bulk solutions α and β and A^w is the effective area of the polarization layers.

Because of the fact that at any point in the transition region the cation flux multiplied by the corresponding cross-sectional area should be equal, when the quasi-stationary state has been reached, we can, with the aid of eqns. (24) and (25), integrate eqn. (19), to yield

$$\frac{-EF}{2t_+^w RT} = \ln \left\{ \frac{c_+^\beta}{c_+^\alpha} \left[\frac{c_+^\beta + \dfrac{J_+ \delta}{D_\pm^w A^w}}{c_+^\alpha - \dfrac{J_+ \delta}{D_\pm^w A^w}} \right]^{(t_+^M/t_+^w)-1} \right\} \quad (26)$$

From eqn. (26) we can see that when thicknesses of the polarization layers approach zero equation becomes

$$E = -2t_+^M \frac{RT}{F} \ln\left(\frac{c_+^\beta}{c_+^\alpha}\right) \quad (27)$$

Equation (27) is usually used to evaluate t_+^M with the EMF method, e.g. in ion-exchange membranes the porosity of which is so low that practically no polarization takes place.

The problem is that the cation flux in eqn. (26) is difficult to measure. To solve this problem we eliminate J_+ using the Donnan equilibrium. According to eqn. (7b) we can in our case express the cation concentration in the membrane as follows:

α-phase side:

$$c_+^B(x=0) = (1-\theta)^{1/2} c_+^\alpha(x=0) \quad (28)$$

β-phase side:

$$c_+^B(x=l) = (1-\theta)^{1/2} c_+^\beta(x=l) \quad (29)$$

Using eqns. (24), (25), (28) and (29) we can write eqn. (26) as

$$\frac{-EF}{2t_+^w RT} = \ln \left\{ \frac{c_+^\beta}{c_+^\alpha} \left[\frac{c_+^\beta + \dfrac{D_\pm^M \dfrac{A^M}{A^w}(1-\theta)^{1/2}(c_+^\alpha - c_+^\beta)\delta}{D_\pm^w l + D_\pm^M \dfrac{A^M}{A^w}(1-\theta)^{1/2} 2\delta}}{c_+^\alpha - \dfrac{D_\pm^M \dfrac{A^M}{A^w}(1-\theta)^{1/2}(c_+^\alpha - c_+^\beta)\delta}{D_\pm^w l + D_\pm^M \dfrac{A^M}{A^w}(1-\theta)^{1/2} 2\delta}} \right]^{(t_+^M/t_+^w)-1} \right\}$$

$$= \ln \left\{ \frac{c_+^\beta}{c_+^\alpha} \left[\frac{c_+^\beta + \dfrac{P^M(c_+^\alpha - c_+^\beta)\delta}{D_\pm^w l + P^M 2\delta}}{c_+^\alpha - \dfrac{P^M(c_+^\alpha - c_+^\beta)}{D_\pm^w l + P^M 2\delta}} \right]^{(t_+^M/t_+^w)-1} \right\} \quad (30)$$

Eqns. (20) and (30) makes it possible to evaluate the parameters $P^M = D_\pm^M A^M / A^w (1-\theta)^{1/2}$ and t_+^M.

In the present discussion we demonstrate a simple way to combine the measured t_+^M and the surface charge density by applying a microscopic treatment. Using the definition of transport number we can write

$$t_+^M(r) = \frac{z_+ J_+ F}{I} = \frac{z_+^2 F^2 c_+(r) u_+ E_z}{F^2[u_+ c_+(r) + u_- c_-(r)] E_z} \quad (31)$$

where I is the electric current density, E_z is the axial electric field strength at a distance r from the pore axis, u_+ is the mobility of the cation and u_- is the mobility of the anion.

When using potassium chloride, which has almost equal ionic diffusivities for the cation and anion, as a base electrolyte we can write eqn. (31) in the form

$$t_+^M(r) = \frac{c_+(r)}{c_+(r) + c_-(r)} \quad (32)$$

Radial concentration profiles of the ions $c_-(r)$ and $c_+(r)$ inside the pore can be expressed using a Boltzmann distribution law

$$c_+(r) = c_+^B \exp(-\psi e/kT) \quad (33)$$

and

$$c_-(r) = c_-^B \exp(\psi e/kT) \quad (34)$$

The electrostatic potential Ψ inside the cylindrical capillary with uniform surface charge density is given,[24] after linearizing the Poisson–Boltzmann equation, as

$$\psi(r/\lambda, x) = \frac{q_2 \lambda}{\varepsilon} \frac{I_0(r/\lambda)}{I_1(r_0/\lambda)} \quad (35)$$

In the space-charge model, both the coion and counter-ion concentrations vary with radial and axial position in the pore. In the present discussion we reject the axial concentration profile and we study the radial concentra-

tion distribution only at one point x in the axial direction; it is reasonable to take this point to be the one which corresponds to the lowest concentration. An approximate expression for t_+^M is obtained by averaging $t_+^M(r)$ over the cross-sectional area of a pore

$$t_+^M = \frac{1}{r_0}\int_0^{r_0} t_+(r)\,dr \qquad (36)$$

which can be integrated together with eqns. (32)–(35) using a numerical method. This simple microscopic model makes it possible to evaluate t_+^M from the surface charge density measured by the streaming potential. The pore radius of a swollen membrane can be estimated by calculating t_+^M with different r_0 values and comparing them with the measured t_+^M.

Experimental

Streaming potential. For this work we developed an automatic streaming potential apparatus based on the one presented in Ref. 25. A new feature of the apparatus was computer control of the pressure difference across the membrane. The computer we used was an ordinary IBM XT model compatible with a data acquisition card (Singular Technology Corp., SC-1402). The variable bidirectional pressure difference was achieved by using two D/A channels to control the peristaltic pump (Ismatec IPS). With this modification both sensitivity and accuracy could be increased by increasing the number of measured points.

The electric potential difference was measured with Ag/AgCl electrodes[26] using an amplifier circuit (Analog Devices Inc. AD202J). The pressure difference was measured with a pressure sensor (SenSym SCX05DNC) which was calibrated for a range of ± 20 kPa using a U-tube manometer with nonlinearity less than 0.2%. A National Semiconductor LM35C sensor was used for temperature measurement and a Philips PW9501 conductivity meter for bulk solution conductivity measurement. All signals were amplified with AD624 (Analog Devices Inc.) instrumentation amplifiers for ± 6 V fixed scale inputs. The solution reservoir was mounted in a thermostatted bath. The sensitivity of each measurement was limited by the detection limit for changes in ΔU, which was about 1 μV when the cell was properly shielded with a Faraday cage. A diagram of the experimental setup is shown in Fig. 2.

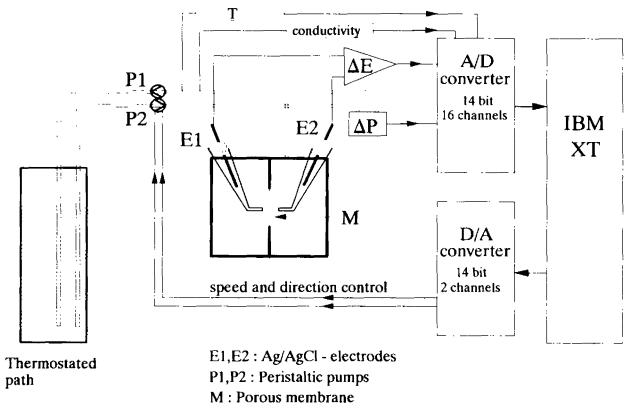

Fig. 2. Schematic drawing of the apparatus for streaming potential measurements used in this work.

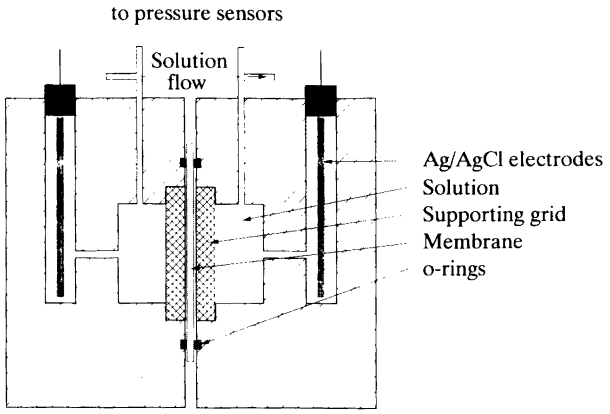

Fig. 3. Side view of the streaming potential cell. Supporting grids are so coarse-meshed that they develop negligible pressure drop and streaming potential compared to the porous membrane.

The cell used in this work was made of PVC. The sideview of the cell is presented in Fig. 3. The electrodes were located in separate compartments and were connected with capillaries to the rest of the cell. Using this arrangement it was possible to avoid contamination on electrode surfaces while monitoring the effect of protein on membrane surface charge density. The membrane was fixed between coarse supporting grids and sealed with O-rings. The area of membranes studied with this cell was 2.5 cm^2.

Each measurement consisted a linear triangle wave of the flow rate from zero to the maximum rates in both

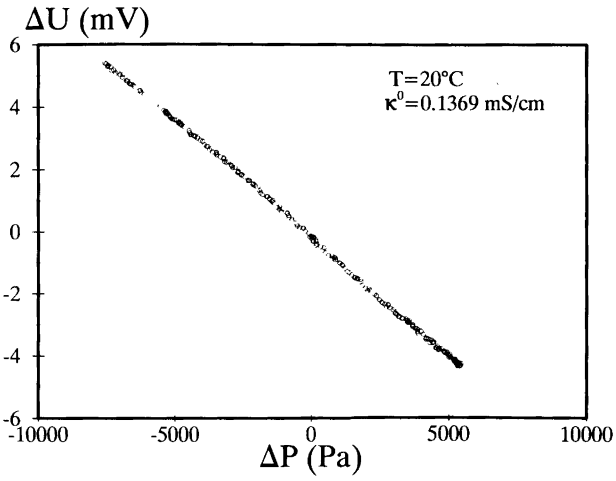

Fig. 4. Data collected during one streaming potential measurement (Durapore membrane, $r_0 = 0.05$ um in 1 mM KCl solution).

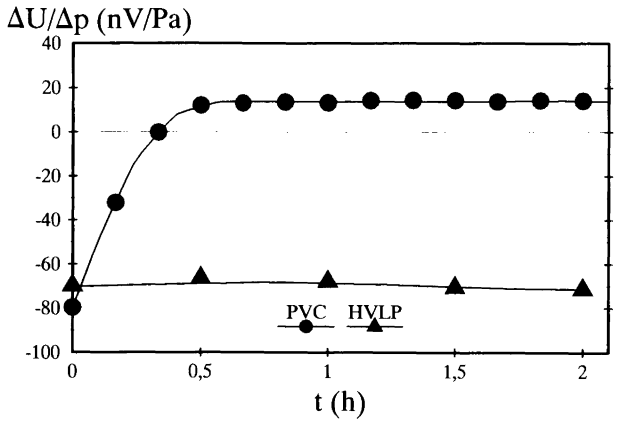

Fig. 5. Example of using a streaming potential measurement to determine the kinetics of protein adsorption on a porous membrane (PVC and HVLP membranes in 10 mM KCl). The zero point on the time scale is fixed to the protein (cytochrome c, 1 g dm^{-3}) injection into the solution of the cell. Before protein injection the membrane was equilibrated with same KCl solution.

directions and back to zero. During the cycle, pressure and potential differences as well as temperature and conductivity were measured 128 times. Using an on-line bunching filter with 12 times oversampling for ΔU and ΔP one cycle lasted about 6 min. As an example, a plot of such measurement is shown in Fig. 4. The apparatus allows much faster measurements by using a lower number of measured points in one cycle, but because the typical time constant of the build-up for phenomena itself is about 1 min,[27] a relatively small improvement in measuring time can be achieved. An example of using this approach in a slow (duration of several minutes) kinetic study is presented in Fig. 5. In this case the membrane was equilibrated in an electrolyte solution until no changes in streaming potential were detected. Protein (cytochrome-c, 1 g dm^{-3}) was injected to the cell, and the adsorption was followed using the streaming potential.

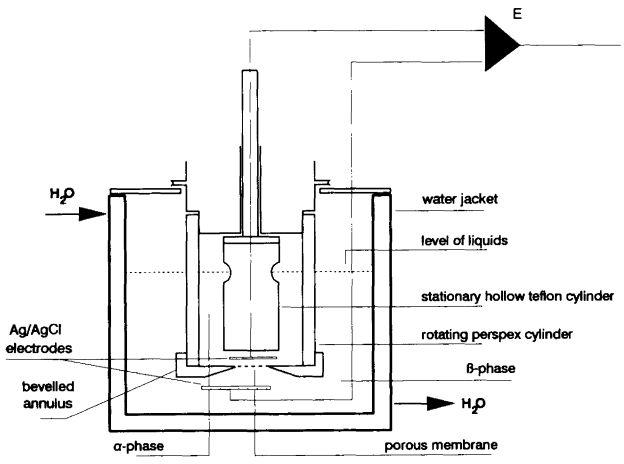

Fig. 6. Rotating diffusion cell.

Transport number by the EMF method. In this work an Oxford Electrodes rotating diffusion cell (Fig. 6) was employed. The membrane was mounted directly onto a bevelled annulus which was screwed to the rotating cylinder. The angle of the bevel is small enough to give appropriate hydrodynamic conditions. This was checked by glueing an MF-Millipore membrane to the rotating cylinder and collapsing part of the membrane surface to produce a well defined surface area.[28] There were no significant differences in the results obtained with these two different procedures. The reversible Ag/AgCl electrodes were placed near the membrane surface as shown in Fig. 6. External noise was reduced by inserting the cell into a Faraday cage.

The cell potential was measured with a pH meter (Radiometer PHM64) and recorded by an x–t recorder. The EMF was measured as function of rotation rate from 1 to 8 Hz in steps of 1 Hz. The measurements were carried out in descending order of rotation rates to reduce the effect of changes in solution concentrations due to diffusion through the membrane.

Measurements

The microfiltration membranes used in the present work were from Millipore. Measurements were made with three different types of membrane: hydrophilic Durapore (polyvinylidene difluoride), MF-Millipore (mixed esters of cellulose) and PVC. Mean pore diameters (d) were 0.10, 0.45, 0.65 and 5.0 μm for Durapore membranes, 0.22, 0.45, 1.2, 3.0 and 8.0 μm for MF-Millipore and 2.0 μm for the PVC membrane. The electrolyte used was KCl (Merck, pro analysis grade) at concentrations 4.5×10^{-5} to 0.1 mol dm^{-3}. All measurements were made at pH 5.8.* Before each experiment the membranes were rinsed with water and equilibrated for 12 h with a similar electrolyte solution as used in the experiments. All measurements with different electrolyte concentrations were then carried out with same piece of membrane. The protein used in adsorption studies was cytochrome c supplied by Sigma Chemical Co. (C-2506) at the concentrations 0.25 and 1.0 g dm^{-3}.

The transport numbers of K^+ in Durapore membranes ($d = 0.1$, 0.45, 0.65 and 5.0 μm), MF-Millipore membrane ($d = 0.22$ μm) and PVC membrane ($d = 2.0$ μm) were determined by the EMF method at 3–6 different KCl concentrations between 4.5×10^{-5} and 9.1×10^{-3} mol dm^{-3}. The β-compartment of the rotating diffusion cell (Fig. 6) was filled with the solution in which the membrane was pre-equilibrated. The concentration in the α-compartment (c^α) was five times higher than c^β in all measurements.

* Solutions were in equilibrium with atmospheric CO_2. Thus $[H^+]$ was constant (1.6×10^{-6} M) throughout the electrolyte solution, and, owing to the thermodynamic analysis, which considers the measuring system to be a binary one, the contribution of H^+ to the transport number is included in the frame of reference of the transport process.

The concentration ratio is a crucial parameter of this method because the sensitivity is directly proportional to it, and t_+^M determined by EMF method describes only integral behaviour over this finite concentration range. The accuracy of the measurement was better than 0.1 mV when a concentration ratio of 5 was used. The membranes for protein adsorption studies were equilibrated with 1 g dm^{-3} cytochrome *c* solution and rinsed well with KCl solution before installation in the rotating diffusion cell. The measurements were carried out with protein-free electrolyte solution to avoid adsorption of protein on the electrodes.

The streaming potentials of the Durapore membranes ($d = 0.1$, 0.45, 0.65 and 5.0 μm), the MF-Millipore membrane ($d = 0.22$ μm) and the PVC membrane were measured at KCl concentrations of 10^{-4}, 10^{-3}, 10^{-2} and 10^{-1} mol dm^{-3}. The measurements with MF-Millipore membranes of other pore diameters ($d = 0.45$, 1.2, 3.0 and 8.0 μm) as well as protein adsorption experiments were carried out in 10^{-2} mol dm^{-3} KCl solution. During the equilibration the streaming potential was followed by repeating the measurement until no drifting was detected. After reaching steady state the result was taken as an average of five measurements with precision better than 2% in 10^{-3} and 10^{-2} mol dm^{-3} solutions and 4% in 10^{-4} and 10^{-1} mol dm^{-3} solutions. Within the same type and pore diameter membrane-to-membrane deviations in q_2 were ±10%. The protein adsorption measurements were carried out by adding the protein directly to the solution in the cell.

Results

Binary electrolyte system (KCl–H_2O). A typical example of direct experimental data obtained from the streaming potential measurements is presented in Fig. 4. From the experimental data the surface charge density (q_2) can be extracted in an iterative manner by using eqns. (16) and (17). By this procedure the results listed in Table 1 were obtained.

The results for the transport numbers in the membrane (t_+^M) measured by the EMF method are shown in Table 2. The iterative procedure used is elucidated in Fig. 7, from which one can deduce that the transport number t_+^M changes the level of cell potential without changing the shape of the curve, while the parameter P^M [eqn. (30)] affects mostly the shape of the curve. Thus it is reasonable to assume that the accuracy of the determination of t_+^M is better than ±0.005.

Protein adsorption. This was studied by the streaming potential and EMF method. The protein, cytochrome c, was added in small amounts (0.25–1.0 g dm^{-3}) into the electrolyte system described above (i.e. to the supporting electrolyte system), and the surface charge density as well as the transport number in the membrane were deter-

Table 1. Measured streaming potentials and the evaluated surface charge densities and effective conductivities.

Membrane	r_0/μm	*c*/mM	$-\Delta U/\Delta p$/nV Pa^{-1}	κ_{eff}/Sm^{-1}	q_2/mC m^{-2}
Durapore SVLP	2.5	0.1	6420	0.001336	−0.290
		1	583	0.01326	−0.817
		10	46.7	0.1277	−1.98
Durapore DVPP	0.325	0.1	11100	0.001838	−0.787
		1	1440	0.01209	−1.91
		10	325	0.1278	−3.11
		100	5.7	0.9291	−5.59
Durapore HVLP	0.225	0.1	6680	0.001349	−0.371
		1	818	0.01331	−1.22
		10	62	0.1278	−2.68
		100	4.07	1.167	−5.02
Durapore VVLP	0.05	0.1	4500	0.001452	−0.586
		1	753	0.01358	−1.47
		10	64.3	0.1281	−3.00
		100	4.56	1.167	−5.75
MF-Millipore	0.11	0.1	3920	0.001348	−0.278
		1	452	0.01317	−0.622
		10	18.2	0.1277	−1.26
		100	2.9	1.167	−3.60
	4	10	60	0.1277	−2.55
	1.5	10	70.5	0.1277	−3.00
	0.6	10	53.2	0.1277	−2.27
	0.225	10	42.3	0.1277	−1.83
PVC	1	0.01	5360	0.000132	−0.0103
		0.1	5250	0.001336	−0.244
		1	920	0.01327	−1.30
		10	94.6	0.1277	−4.03
		100	5.67	1.167	−6.96

Table 2. Results of EMF measurements

Membrane	c/mM	$t_{+(K)}$	$P^M/10^{-5}$ cm^2 s^{-1}
VVLP (0.1 μm)	0.1	0.840	0.8
	0.51	0.748	1.2
	2.5	0.600	1.8
HVLP (0.45 μm)	0.045	0.673	1.5
	0.05	0.639	1.6
	0.5	0.610	1.8
	0.99	0.546	1.9
	4.9	0.500	1.9
	9.1	0.503	1.9
DVPP (0.65 μm)	0.057	0.652	1.5
	0.51	0.550	1.8
	2.5	0.500	1.9
SVLP (5.0 μm)	0.05	0.637	1.6
	0.057	0.545	1.8
	0.39	0.564	1.9
	0.95	0.525	1.9
	5.0	0.524	1.9
PVC (2.0 μm)	0.056	0.635	1.5
	0.1	0.580	1.6
	0.36	0.574	1.7
	0.99	0.550	1.8
	4.9	0.506	1.9
	9.1	0.500	1.9
MF (0.22μm)	0.05	0.805	1.2
	0.39	0.552	1.8
	0.95	0.493	1.8

mined. These determinations were carried out and interpreted as in the case of the binary electrolyte system. This is possible because the molar concentration of the protein remained so low that its contribution was seen only through its effect on the surface charge, i.e. the protein adsorption changes q_2 and t_+^M, but otherwise the protein does not contribute. The results are presented in Tables 3 and 4, for the streaming potential measurements and transport number measurement, respectively.

The streaming potential also proved to be a convenient method to study the transient behaviour of the protein adsorption onto the pores of the porous membranes. An example of these experiments is shown in Fig. 5. A similar, relatively slow adsorption process was detected for all the membranes studied which adsorbed protein. Interestingly, the protein remained adsorbed on the surface of the membrane pores for the period of two days studied after changing the protein-free electrolyte solution in the cell. In fact, this kind of behaviour made it possible to measure the transport numbers by the EMF method,

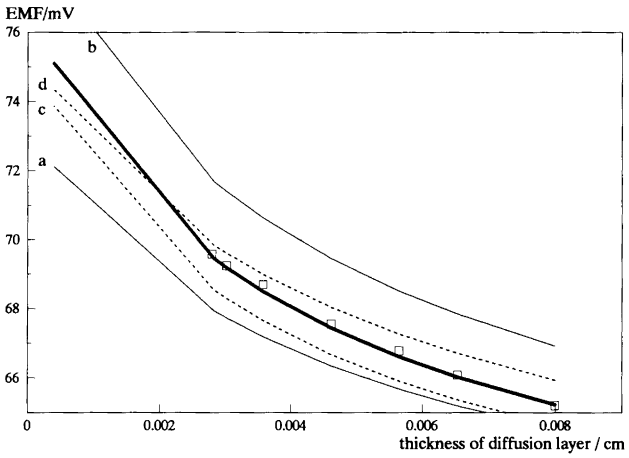

Fig. 7. Example of using eqns. (20) and (30) to fit the measured EMF δ-dependence (□, HVLP in 5.0×10^{-5} mol dm^{-3}). The wide solid line represents the best fit with parameters $t_+^M = 0.639$ and $P^M = 1.6\times10^{-5}$ mol dm^{-3}. The solid lines (a) ($t_+^M = 0.62$) and (b) ($t_+^M = 0.67$) are calculated using $P^M = 5.0\times10^{-5}$ mol dm^{-3}. Dashed lines (c) ($P^M = 2.0\times10^{-5}$ mol dm^{-3}) and (d) ($P^M = 1.4\times10^{-5}$ mol dm^{-3}) are calculated with $t_+^M = 0.639$.

since the membranes could be treated with the protein solutions before putting them into the EMF cell. This is due to the fact that if a protein-containing electrolyte solution were introduced to the cell the silver/silver chloride electrodes would be contaminated by the adsorption of protein on the surface of the electrodes, having an effect on the cell potential.

Discussion

All of the studied polymeric microfiltration membranes appeared to have, in the absence of protein, cation-exchange properties; i.e. the adsorption of anions, in our case chloride ions, took place. A recent study[19] deals with this phenomenon, and proposes the use of the Freudlich adsorption isotherm to explain the results. Therefore, the measured surface charge densities were fitted to this adsorption isotherm; $q_2 = bc^n$ where c is the electrolyte concentration, and b and n are experimental parameters. The results are shown in Table 5. As can be seen, the exponent n is ca. 1/3 for the Durapore and MF-Millipore membranes, and ca. 2/3 for the PVC membrane. These results clearly indicate that the chloride ions are physically adsorbed on the membrane matrix.

Table 3. Results of streaming potential measurements with protein solution.

Membrane	r_0/μm	c_{Cyt}/g dm^{-3}	$-\Delta U/\Delta p$/nV Pa^{-1}	κ_{eff}/Sm^{-1}	q_2/mC m^{-2}
MF-Millipore	0.11	0	79.6	0.1277	−3.40
		0.25	24	0.1277	−1.02
		1.0	15.1	0.1277	−0.640
PVC	1	0	94.6	0.1279	−4.09
		0.25	−10.2	0.1277	0.435
		1.0	−14	0.1277	0.595

Table 4. Results of transport number measurements with protein (1 g dm^{-3}).

Membrane	c/mM	$t_{+(K)}$	$P^M/10^{-5}$ cm^2 s^{-1}
HVLP (0.45 μm)	0.05	0.645	1.6
SVLP (5.0 μm)	0.11	0.557	1.9
	0.39	0.560	1.9
MF (0.22 μm)	0.05	0.431	1.9
	0.1	0.475	1.9
	0.63	0.480	1.9
PVC (2.0 μm)	0.3	0.358	1.8
	1.0	0.445	1.8
	5.0	0.489	1.8

From the values for the surface charge density the distance of adsorbed chloride ions (d_{Cl-Cl}) can be estimated. An estimate for d_{Cl-Cl} is obtained assuming that the adsorbed ions form a squared net on the surface of the pores. In Table 6 we have presented the calculated values for d_{Cl-Cl} together with the Debye length (λ)[20] in different concentrations. As can be seen, in concentrated solutions the charges of the chloride ions are discrete, while in dilute solutions the Debye lengths overlap, forming a more or less uniform charge distribution. Going back to the modelling of the streaming potential and the surface charge density, a discrepancy is evident, viz. in the modelling it is assumed that the charge is uniformly distributed over the surface. In spite of this serious discrepancy the results seem to be adequate, e.g. when considering the above presented fitting of the Freundlich adsorption isotherm. This kind of strange situation has been discussed by McLaughlin, and according to his review article[29] it seems to be so that the effect of the discrete charges (almost always neglected in the theoretical considerations) does not have to be taken into account in all cases, obviously including the present case.

An interesting application of the transport number in porous membranes is the possibility of estimating the average pore size (r_0) of the membrane after swelling and possible adsorption. In the case of wide-pore membranes ($r_0/\lambda > 10$) the surface charge density is practically independent of r_0 [eqn. (16)]. Therefore, the surface charge densities calculated from the streaming potential measurements can be utilized to evaluate r_0 from eqn. (36). Results thus obtained are listed in Table 7. The results are in accordance with the values given by the manufacturer, except for SVLP and PVC membranes with nominal pore sizes (diameters) of 5.0 and 2.0 μm, respectively. In the case of the PVC membrane the reason for the deviation is swelling, and in the case of SVLP the rotation of the membrane is mixing (stirring through the membrane) the solutions because of the high porosity (ca. 80%) and large diameter of the pore. It is important to realize that according to this result the EMF method in a rotating diffusion cell cannot be applied for these large pore membranes, but the limit is approximately in the pore radius of 1 μm. The swelling of PVC membranes was also detected with the aid of flow rate measurements through the membrane; the flow rate decreased continuously after putting the membrane in contact with the solution. The reasonable results obtained for the values of r_0 support the modelling with uniform charge distribution.

Table 6. Estimated distances of adsorbed chloride ions and Debye lengths as a function of electrolyte concentration.

c_{KCl}/mM	λ/nm	d^{Cl-Cl}/nm
100	0.96	5.6
10	3.04	7.07
1	9.6	11.5
0.1	30.4	20.8

Results for protein adsorption indicate that Durapore membranes do not practically adsorb proteins (as reported by the manufacturer) and that PVC and MF membranes do adsorb proteins. In the case of PVC even the sign of the charge in the membrane is changed. As mentioned before, the adsorbed protein cannot be removed from the membrane by putting fresh, protein free, electrolyte solution (at the same concentration as that with the protein) in contact with the membrane. This fact evidently confirms the hydrophobic nature of the interaction between the protein and the membrane matrices. Furthermore, an interesting aspect is the slowness of the adsorption process of the protein, also noticed by Norde *et al.*[30] This phenomenon may be of great importance when trying to find an explanation for protein adsorption on a polymeric matrix. However, so far we have studied only one protein (a simple one), so in order for us to be able to draw conclusions other proteins must be investigated. These studies are now, after the establishment of reliable methods, in progress.

Table 5. Constants for a Freundlich-type isotherm for chloride ion adsorption on the studied membranes.

Membrane	r_0	n	$-10^3 b$
Durapore	2.5	0.417	0.78
	0.325	0.277	1.64
	0.225	0.373	1.02
	0.05	0.327	1.35
MF-Millipore	0.11	0.364	0.62
PVC	1	0.609	1.09

Table 7. Estimated pore sizes of the membranes studied using transport-number data.

Membrane	Pore diameter/μm
VVLP (0.1 μm)	0.1
HVLP (0.45 μm)	0.32
DVPP (0.65 μm)	0.55
SVLP (5.0 μm)	0.3
PVC (2.0 μm)	0.26
MF (0.22 μm)	0.20

As to the initial reason for this study, viz. to determine the limits of use of the concept of an inert porous membrane, we can make the following conclusions. Generally speaking, if the concentration of the supporting electrolyte is ca. 10^{-3} M or larger, the transport process inside the membrane, with pore size varying from 0.1 to 8 μm, can be modelled as in the electrolyte solution. The exact limit is naturally dependent on the pore size; the larger is the pore size, the lower is the concentration limit at which the transport process behaves as in the inert membrane. Furthermore, the pore size is practically unaffected by protein adsorption, because only a monolayer is formed.

Acknowledgments. This work has been supported by TEKES (the Technology Development Centre in Finland).

References

1. Ekman, A., Forssell, P., Kontturi, K. and Sundholm, G. *J. Membr. Sci. 11* (1982) 65.
2. Kontturi, K., Forssell, P. and Ekman, A. *Sep. Sci. Technol. 17* (1982) 1195.
3. Forssell, P. and Kontturi, K. *Sep. Sci. Technol. 18* (1983) 205.
4. Kontturi, K., Ojala, T. and Forssell, P. *J. Chem. Soc., Faraday Trans. 1, 80* (1984) 3379.
5. Kontturi, K. *Sep. Sci. Technol. 21* (1986) 591.
6. Kontturi, K. and Pajari, H. *Sep. Sci. Technol. 21* (1986) 1089.
7. Kontturi, K. *Sep. Sci. Technol. 23* (1988) 227.
8. Kontturi, K. and Westerberg, L. M. *Sep. Sci. Technol. 23* (1988) 235.
9. Kontturi, K. and Revitzer, H. *Sep. Sci. Technol. 24* (1989) 453.
10. Kontturi, A. K., Kontturi, K., Savonen, A., Schiffrin, D. J. and Vuoristo, M. *J. Chem. Soc., Faraday Trans. 89* (1993) 99.
11. Kontturi, A. K. and Kontturi, K. *J. Colloid Interface Sci. 120* (1987) 256.
12. Kontturi, A. K. and Kontturi, K. *J. Colloid Interface Sci. 124* (1988) 328.
13. Kontturi, A. K. and Kontturi, K. *Acta Polytechn. Scand. 178* (1987) 143.
14. Kontturi, A. K. *J. Chem. Soc., Faraday Trans. 1, 84* (1988) 4033.
15. Kontturi, A. K., Kontturi, K. and Niinikoski, P. *J. Chem. Soc., Faraday Trans. 86* (1990) 3097.
16. Kontturi, A. K., Kontturi, K. and Niinikoski, P. *J. Chem. Soc., Faraday Trans. 87* (1991) 1779.
17. Kontturi, A. K., Kontturi, K., Niinikoski, P., Savonen, A. and Vuoristo, M. *Acta Chem. Scand. 46* (1992) 348.
18. Kontturi, A. K., Kontturi, K., Niinikoski, P. and Murtomäki, L. *Acta Chem. Scand. 46* (1992) 941.
19. Manzanares, J. A., Mafé, S. and Ramírez, P. *J. Non-Equilib. Thermodyn. 16* (1991) 255.
20. Newman, J. S. *Electrochemical Systems*, Prentice-Hall Inc., Englewood Cliffs, NJ 1973.
21. Westermann-Clark, G. B. and Anderson, J. L. *J. Electrochem. Soc. 130* (1983) 839.
22. Ekman, A., Liukkonen, S. and Kontturi, K. *Electrochimica Acta 23* (1978) 243.
23. Albery, W. J., Burke, J. F., Leffler, E. B. and Hadcraft, J. *J. Chem. Soc., Faraday Trans 1, 72* (1976) 1618.
24. Sørensen, T. S. and Koefoed, J. *J. Chem. Soc., Faraday Trans 2, 70* (1974) 665.
25. Nyström, M., Lindström, M. and Matthiasson, E. *Colloid Surf. 36* (1989) 297.
26. Ives, D. J. G. and Janz, G. J. *Reference Electrodes*, Theory and Practice, Academic Press, NJ 1961.
27. Kumar, R. and Singh, K. *Ind. J. Chem., Sect. A 19* (1980) 511.
28. Albery, W. J., Choudhery, R. A. and Fisk, P. R. *Faraday Discuss. Chem. Soc. 77* (1984) 53.
29. McLaughlin, S. *Annu. Rev. Biophys. Chem. 18* (1989) 113.
30. Norde, W. and Rouwendal, E. *J. Colloid Interface Sci. 139* (1990) 169.

Received February 26, 1993.